

See discussions, stats, and author profiles for this publication at: <https://www.researchgate.net/publication/265689357>

Flux-gate magnetometer spin axis offset calibration using the electron drift instrument

Article in Measurement Science and Technology · September 2014
DOI: 10.1088/0957-0233/25/10/105008

CITATIONS
7

READS
69

8 authors, including:



Rumi Nakamura
Austrian Academy of Sciences
586 PUBLICATIONS 12,320 CITATIONS

SEE PROFILE



Hannes Karl Leinweber
University of California, Los Angeles
52 PUBLICATIONS 1,521 CITATIONS

SEE PROFILE

Some of the authors of this publication are also working on these related projects:



International Magnetospheric Studies IMS [View project](#)



SOSMAG AMR sensors for the KSEM satellite [View project](#)

Flux-gate magnetometer spin axis offset calibration using the electron drift instrument

Ferdinand Plaschke¹, Rumi Nakamura¹, Hannes K Leinweber², Mark Chutter³, Hans Vaith³, Wolfgang Baumjohann¹, Manfred Steller¹ and Werner Magnes¹

¹ Space Research Institute, Austrian Academy of Sciences, Graz, Austria

² Department of Earth and Space Sciences, University of California Los Angeles, Los Angeles, CA, USA

³ University of New Hampshire, Durham, NH, USA

E-mail: ferdinand.plaschke@oeaw.ac.at

Received 9 April 2014, revised 22 July 2014

Accepted for publication 29 July 2014

Published 15 September 2014

Abstract

Spin-stabilization of spacecraft immensely supports the in-flight calibration of on-board flux-gate magnetometers (FGMs). From 12 calibration parameters in total, 8 can be easily obtained by spectral analysis. From the remaining 4, the spin axis offset is known to be particularly variable. It is usually determined by analysis of Alfvénic fluctuations that are embedded in the solar wind. In the absence of solar wind observations, the spin axis offset may be obtained by comparison of FGM and electron drift instrument (EDI) measurements. The aim of our study is to develop methods that are readily usable for routine FGM spin axis offset calibration with EDI. This paper represents a major step forward in this direction. We improve an existing method to determine FGM spin axis offsets from EDI time-of-flight measurements by providing it with a comprehensive error analysis. In addition, we introduce a new, complementary method that uses EDI beam direction data instead of time-of-flight data. Using Cluster data, we show that both methods yield similarly accurate results, which are comparable yet more stable than those from a commonly used solar wind-based method.

Keywords: flux-gate magnetometer, electron drift instrument, in-flight calibration, spin axis offset

(Some figures may appear in colour only in the online journal)

1. Introduction

The *in-situ* characterization of the magnetic field in space has been a major objective of numerous spacecraft missions. For that purpose, flux-gate magnetometers (FGMs) are commonly used due to their superior accuracy, stability, and robustness, paired with their relatively low mass and power demand, e.g. [1, 4].

The primary output of FGMs are raw vectorial magnetic field measurements \mathbf{B}_{raw} in sensor coordinates. These need to

be transformed into physically meaningful units and coordinate systems, e.g. with the following equation:

$$\mathbf{B} = \mathbf{G} \cdot \mathbf{M} \cdot \mathbf{B}_{\text{raw}} - \mathbf{O} \quad (1)$$

Here, \mathbf{B} represents the calibrated magnetic field measurements, \mathbf{M} is a 3×3 matrix dependent on six angles that transforms from sensor coordinates to an orthogonal, spacecraft-fixed coordinate system, \mathbf{G} is a diagonal matrix consisting of three gain parameters, and \mathbf{O} is a 3D offset vector. Altogether, \mathbf{M} , \mathbf{G} , and \mathbf{O} are dependent on 12 parameters (6 angles, 3 gains, and 3 offsets) that have to be determined by ground-based (pre-launch) or in-flight (post-launch) calibration procedures, e.g. [3, 9, 11, 21].



Content from this work may be used under the terms of the [Creative Commons Attribution 3.0 licence](https://creativecommons.org/licenses/by/3.0/). Any further distribution of this work must maintain attribution to the author(s) and the title of the work, journal citation and DOI.

The vector \mathbf{O} may exhibit larger variations due to spacecraft contributions: the vector represents the FGM measurement in zero ambient field, i.e. to a major extend, the stray fields of the spacecraft on which the FGM is mounted. These fields result from remanently magnetized parts and/or electric currents, e.g. [14]. Changes thereof that directly affect \mathbf{O} can only be accounted for by in-flight calibration.

Fortunately, the in-flight calibration procedures are relatively easy for spacecraft that are spin-stabilized. In that case, 8 of the 12 calibration parameters influence the measurements' spectral power at spacecraft spin frequency and/or harmonics in any inertial (de-spun) coordinate system, e.g. [2], which facilitates their in-flight determination. Out of these eight parameters, two are the spin plane components of \mathbf{O} , which we denote as O_y and O_z . However, determining the spin axis offset O_x (spin axis in x direction) is much more difficult.

Usually, O_x is obtained by analyzing solar wind (SW) FGM measurements that contain Alfvénic disturbances, i.e. field rotations without changes in field strength, e.g. [10, 13, 18]. Alternatively, simultaneous observations from an electron drift instrument (EDI) may be used. EDI consists of two gun-detector units (GDUs) mounted on opposite sides of a spacecraft. Each GDU can emit modulated electron beams. The electrons perform one (or more) gyrations in the ambient magnetic field and are registered by the other GDU. The electron time-of-flight (TOF) T is in principle inversely proportional to the field strength:

$$|\mathbf{B}| = \frac{2\pi m_e}{eT} = \frac{k}{T} \quad (2)$$

Here, m_e is the relativistic electron mass, e is the elementary charge, and $k = 2\pi m_e/e$. Differences in T as measured by both GDUs indicate the presence of an electric field or magnetic field gradient [17, 19]. Since measurements of $|\mathbf{B}|$ by an EDI are independent from spacecraft stray fields, they can be used to determine O_x : A correction to this offset is given by the difference between FGM and EDI measured $|\mathbf{B}|$, if the field points in spin axis direction. In this paper, we denote such a method of determining or adjusting O_x via EDI TOF measurements as time-of-flight method (TOF method).

An early description of the TOF method can be found in [8]. Later [12] explored the possibility of determining some of the parameters of matrix \mathbf{G} by a comparison of FGM and EDI measurements. Just recently [15] showed that the EDI TOF data are also subject to offsets, which systematically alter the O_x results by the TOF method. These studies proved the feasibility of the TOF method, but fell short of presenting a mature method for FGM spin axis offset determination using EDI measurements, which takes into account TOF offsets and other inaccuracies in FGM and EDI observations.

The importance of such a method and timeliness of its development is rooted in its relevance for NASA's upcoming Magnetospheric Multi-Scale (MMS) mission. The mission consists of four spacecraft (featuring FGM and EDI instruments) that will explore the Earth's magnetosphere. The primary objective of the mission is to investigate the physics of magnetic reconnection. During the first years of operation, the MMS spacecraft will rarely encounter the pristine SW, if at all,

as their apogee distances from Earth will be too low. Hence, MMS will rely on the availability of a working, mature, EDI-based method for spin axis offset calibration.

The purpose of this paper is to make a major step forward in the development of such a method. First, we provide the TOF method with a comprehensive error analysis that facilitates the determination of spin axis offsets with higher accuracy. Secondly, we introduce another, complementary method which makes use of EDI beam direction (BD) data instead of TOF data. Consequently, we denote this method as beam direction method (BD method). Finally, we compare the spin axis offset results of the TOF method, of the BD method, and of a typically used solar wind (SW) based method [13], which is henceforth denoted as SW method. The data set we base this comparison on consists of one year (2008) of Cluster 3 FGM and EDI measurements.

2. Methods

Apart from the spin axis offset O_x , we assume the FGM measurements to be well-calibrated. Furthermore, we assume that for every EDI measurement there is a simultaneous FGM observation \mathbf{B} available. We would like to point out that the methods described in this section provide spin axis offsets O_x after equation (1) if the FGM observations \mathbf{B} are initially computed from \mathbf{B}_{raw} using $O_x = 0$. Otherwise, O_x denotes a correction to the already applied spin axis offset rather than the entire offset itself.

2.1. TOF method

Step 1: In order to avoid systematic errors in O_x , the EDI GDU and operation mode dependent TOF offsets have to be corrected first, as shown by Nakamura et al [15]. For this purpose, measurements need to be selected for which $|\mathbf{B}|$ is unaffected by O_x (magnetic field close to the spin plane, i.e. y - z -plane):

$$\frac{|B_x|}{|\mathbf{B}|} < C_{\text{sp}} \quad (3)$$

Here C_{sp} is a threshold value; B_x and $|\mathbf{B}|$ are FGM-measured quantities. From the selected FGM and simultaneous EDI data, differences δT between FGM-determined magnetic field strengths, converted to TOFs, and EDI measured TOFs are computed:

$$\delta T = T - \frac{k}{|\mathbf{B}|} \quad (4)$$

Therewith, we obtain one TOF offset O_T per GDU and operation mode:

$$O_T = \text{median}(\delta T) \pm \Delta O_T \quad (5)$$

$$\Delta O_T = \text{stddev}(\delta T) \quad (6)$$

Note that O_T is specific to each GDU and operation mode. Hence, for the computation of each offset O_T only samples δT corresponding to the particular GDU and obtained when the instrument was in the respective mode may be used.

Step 2: All TOF values T (belonging to a particular GDU and mode, not restricted by C_{sp}) are subsequently corrected with the corresponding TOF offsets O_T :

$$T_c = T - O_T \pm \Delta T_c \quad (7)$$

$$\Delta T_c = \Delta O_T \quad (8)$$

Therewith, estimates of the FGM spin axis offset (correction) O_x can be computed:

$$O_x = B_x - \text{sign}(B_x) \sqrt{\frac{k^2}{T_c^2} - B_y^2 - B_z^2} \pm \Delta O_x \quad (9)$$

The uncertainty ΔO_x of each O_x estimate does not only stem from ΔT_c , i.e. from the TOF offset computations, but also from the inherent FGM measurement and calibration uncertainty of \mathbf{B} . Inaccuracies in \mathbf{G} and \mathbf{M} will result in errors of \mathbf{B} that scale with the strength of the magnetic field. Furthermore, there is a FGM noise floor which defines a minimum uncertainty of \mathbf{B} . Taking both uncertainties into account, we assume each component of \mathbf{B} to be associated with an error of the following form:

$$\Delta B = |\mathbf{B}| \Delta g + \Delta B_n \quad (10)$$

where Δg is a factor of unit 1 and ΔB_n is the noise level in nT. From equations (9) and (10) we derive the error of O_x (error propagation):

$$\Delta O_x = \sqrt{\frac{k^2}{T_c^2} \left[\Delta B^2 + \frac{k^2 \Delta T_c^2}{T_c^4} \right]} \quad (11)$$

As can be easily seen, ΔO_x increases with the factor:

$$\sqrt{\frac{\frac{k^2}{T_c^2}}{\frac{k^2}{T_c^2} - B_y^2 - B_z^2}} \approx \frac{|\mathbf{B}|}{|B_x|} \quad (12)$$

Consequently, it is advantageous for spin axis offset determinations with the TOF method if the field is low in strength and directed along the spin axis.

Step 3: The samples of O_x (and corresponding ΔO_x) are the basis for the computation of a final offset (correction) value O_{xf} for a specific time interval of length t_{int} . Therefore, we select those O_x within the time interval, for which $\Delta O_x \leq C_O$ holds (C_O is a threshold value), and compute:

$$O_{xf} = \text{median}(O_x) \quad (13)$$

with upper/lower error bounds given by the 16th and 84th percentiles $O_{xf} - \Delta O_{xf-}$ and $O_{xf} + \Delta O_{xf+}$ of the distribution of selected/contributing O_x , if their number exceeds another threshold number $C_{\#}$. The percentiles yield a 2σ range around the mean, if the estimates O_x are normally distributed, but also account for skewness of the distribution. The average error of O_{xf} is given by:

$$\begin{aligned} \langle \Delta O_{xf} \rangle &= \frac{1}{2} [(O_{xf} + \Delta O_{xf+}) - (O_{xf} - \Delta O_{xf-})] \\ &= \frac{\Delta O_{xf+} + \Delta O_{xf-}}{2} \end{aligned} \quad (14)$$

Clearly, the choice of t_{int} , C_O , and $C_{\#}$ will influence the result O_{xf} . Larger intervals increase the statistical basis at the expense of a larger spread of the O_x estimates due to offset drift. Lowering C_O and increasing $C_{\#}$ will also increase the

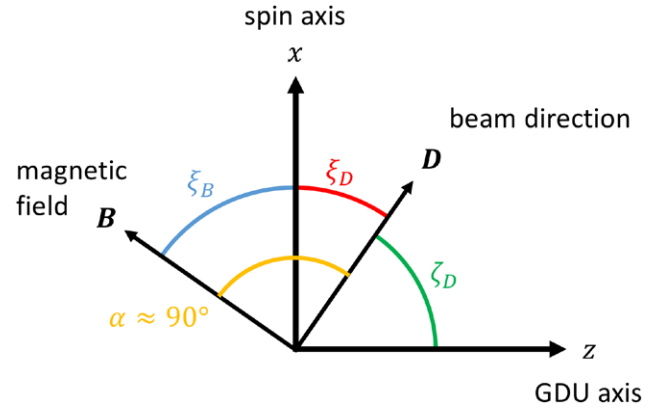


Figure 1. Sketch illustrating the angles between distinguished directions. Note that \mathbf{B} and \mathbf{D} have non-vanishing y-components (out of the figure plane), in general.

quality of O_{xf} in general, but less intervals of length t_{int} may fulfill the criteria and yield such an offset value.

It should be noted that realistic uncertainties ΔO_x facilitate the selection of the most accurate estimates O_x for the computation of a final offset (correction) O_{xf} . Hence, error analysis is not only necessary to assess the uncertainty of any result, but is also crucial, in this case, for maximizing the result's accuracy.

2.2. BD method

Only those electron beams, that are emitted by an EDI GDU perpendicular to the ambient magnetic field, are able to return to the spacecraft. Hence, EDI beam directions (BD), which we denote with \mathbf{D} , should be perpendicular to \mathbf{B} . Deviations in angles α (depicted in orange in figure 1) between FGM measured \mathbf{B} and EDI measured \mathbf{D} from 90° may be attributed to inaccuracies in spin axis offset O_x .

Step 1: BDs are not subject to TOF offsets. However, for any BD method to yield accurate spin axis offsets, the coordinate systems of the BDs and of the calibrated FGM data have to coincide. Any adjustment of the coordinate systems should be based on FGM and EDI measurements for which the angles α are least affected by the spin axis offset (\mathbf{D} close to the spin plane). Our selection criterion is:

$$\frac{|D_x|}{|\mathbf{D}|} = |D_x| < C_{sp} \quad (15)$$

where $|\mathbf{D}| = 1$. Therewith, GDU specific coordinate transformations for the EDI BDs are found by minimization of the mean of $(\alpha - 90^\circ)^2$. The standard deviation

$$\Delta\beta = \text{stddev}(\alpha - 90^\circ) \quad (16)$$

can be regarded as angular uncertainty of the BD vectors \mathbf{D} . The target coordinate systems should ideally coincide with the coordinate system of the calibrated FGM measurements. All the EDI BDs \mathbf{D} (not restricted by C_{sp}) are transformed into these systems.

Step 2: Ideally, $\mathbf{B} \cdot \mathbf{D} = 0$, as stated above. Deviations can be attributed to the FGM spin axis offset as follows:

$$O_x = \frac{\mathbf{B} \cdot \mathbf{D}}{D_x} \pm \Delta O_x \quad (17)$$

Table 1. TOF offsets and uncertainties $O_T \pm \Delta O_T$ (in μs) dependent on GDU (1 or 2) and EDI mode (code length f and clock dividers n and m).

n	m	$O_T \pm \Delta O_T (\mu\text{s})$			
		GDU 1		GDU 2	
		$f=0$	$f=1$	$f=0$	$f=1$
1	8	—	—	—	—
2	8	—	—	—	—
4	8	-0.412 ± 1.330	—	-0.955 ± 1.110	-0.459 ± 1.273
8	8	-0.885 ± 1.747	—	-1.415 ± 1.752	—
16	8	-0.142 ± 3.649	—	-0.898 ± 3.629	—
32	8	-1.004 ± 3.228	—	-1.252 ± 8.972	—
1	16	0.006 ± 0.103	-0.018 ± 0.206	-0.259 ± 0.188	-0.245 ± 0.191
2	16	—	-0.059 ± 0.406	-1.117 ± 1.067	-0.289 ± 0.439
4	16	—	-0.435 ± 1.149	—	-0.522 ± 1.118
8	16	-0.477 ± 0.693	-0.264 ± 2.699	-0.684 ± 0.903	-0.535 ± 2.673
16	16	—	0.107 ± 4.503	—	-0.246 ± 6.329
32	16	—	—	—	3.327 ± 19.23

Here, the uncertainty ΔO_x results from the uncertainties of the components of \mathbf{B} (after equation (10)) and of the components of \mathbf{D} :

$$\Delta D = \sin(\Delta\beta) \quad (18)$$

Note that $\Delta\beta$ and, hence, ΔD are GDU specific. Therewith, we obtain the error in O_x in a similar manner to equation (11):

$$\Delta O_x = \sqrt{\frac{\Delta B^2}{D_x^2} + \frac{\Delta D^2}{D_x^2} \left[\frac{(B_y D_y + B_z D_z)^2}{D_x^2} + B_y^2 + B_z^2 \right]} \quad (19)$$

Here ΔB and ΔD are computed in accordance to equations (10) and (18), and $|\mathbf{D}| = 1$. As can be seen, ΔO_x increases with decreasing D_x^2 and also with increasing $|\mathbf{B}|^2$, as:

$$\frac{(B_y D_y + B_z D_z)^2}{D_x^2} + B_y^2 + B_z^2 \approx \frac{(B_x D_x)^2}{D_x^2} + B_y^2 + B_z^2 = |\mathbf{B}|^2 \quad (20)$$

The reason for this behavior stems from the sensitivity of α to changes in O_x being given by the quotient of the two quantities D_x^2 and $|\mathbf{B}|^2$:

$$\left(\frac{\partial \alpha}{\partial O_x} \right)^2 = \frac{D_x^2}{|\mathbf{B}|^2} \quad (21)$$

Consequently, it is advantageous for spin axis offset determinations with the BD method if the field is low in strength and pointing in perpendicular direction to the spin axis.

Step 3: Following the description of step 3 of the TOF method, a final spin axis offset (correction) value O_{xf} for a time interval of length t_{int} can be computed from O_x estimates pertaining to that interval, for which $\Delta O_x < C_O$ holds, via:

$$O_{xf} = \text{median}(O_x) \quad (22)$$

if their number exceeds a minimum threshold of $C_{\#}$. Upper/lower error bounds $O_{xf} - \Delta O_{xf-}$ and $O_{xf} + \Delta O_{xf+}$ may again be given by the 16th and 84th percentiles of the distribution of selected/contributing O_x , with equation (14) defining the average error $\langle \Delta O_{xf} \rangle$ of the final spin axis offsets (or offset corrections) O_{xf} .

2.3. SW method

Magnetic field fluctuations embedded in the solar wind (SW) are primarily Alfvénic in nature, i.e. the field changes rather in direction than in magnitude. Hence, the magnitude of the magnetic field tends to be more constant over time than any of its three components [16]. The spin axis offset of a FGM can be determined in the solar wind by making use of this property, as incorrect offsets lead to an artificial increase in fluctuation levels of the field magnitude [1, 5, 6, 10, 20]. The technique used herein introduced and described in [13] is an improved and automated version of the Davis–Smith method [6]. Henceforth, it is referred to as SW method. This method relies on a few hours of FGM solar wind data as input, and yields final spin axis offset (correction) values O_{xf} (O_3 in [13]) as well as upper and lower error bounds $O_{xf} - \Delta O_{xf-}$ and $O_{xf} + \Delta O_{xf+}$ ($O_{3\text{min}}$ and $O_{3\text{max}}$ in [13]), just as the TOF and BD methods.

3. Application

We apply the TOF, the BD, and the SW methods to one year (2008) of Cluster 3 EDI and FGM measurements. The FGM measurements were calibrated using the daily calibration files [7]. Roughly 25 million EDI data samples (i.e. combinations of \mathbf{D} , T , as well as corresponding simultaneous FGM measurements \mathbf{B}) are available for that year.

It should be noted that the daily calibration files include a non-vanishing spin axis offset, which remains constant throughout the year 2008. Consequently, all values O_x that are determined by the TOF, the BD, and the SW methods are corrections to that daily calibration file spin axis offset.

3.1. TOF method

Step 1 consists of the determination of GDU and EDI mode dependent TOF offsets. For this task, we selected EDI and FGM measurements in accordance to equation (3) with $C_{\text{sp}} = 0.1$. Two oppositely directed GDUs are placed on each Cluster spacecraft. The mode of each of these units is characterized by three parameters: n , m , and the code flag f . These parameters control the pseudo noise sequence of electrons emitted by

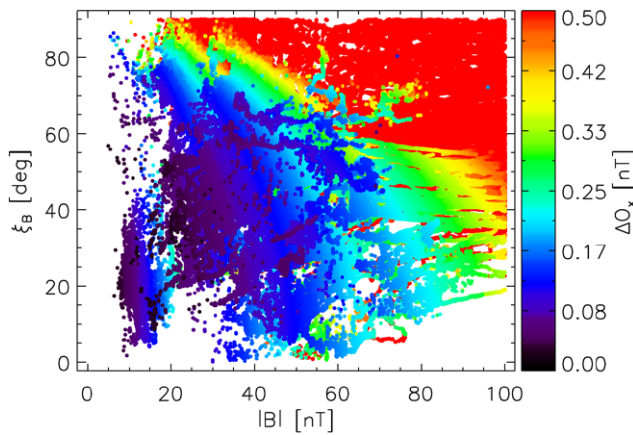


Figure 2. ΔO_x , resulting from the application of the TOF method to Cluster 3 EDI and FGM measurements from 2008, as a function of $|B|$ and the angle ξ_B between B and the spin axis x .

each GDU. A sequence may consist of either 15 (short code, $f=0$) or 127 chips (long code, $f=1$). The chip length is given by the product of n and m , which are dividers of the internal EDI clock. Although EDI can in principle emit electrons at different energies, only one energy level was used (1 keV). The corresponding relativistic conversion factor between TOF and magnetic field values is $k = 35\,793.785\,\mu\text{s nT}$ [17].

During 2008, both Cluster 3 GDUs were operated in modes characterized by $n \in [1, 2, 4, 8, 16, 32]$ and $m = 8$ or 16. As EDI is a system of 2 GDUs, each being able to emit modulated electron beams with 2 different code lengths, with chip lengths given by 6×2 combinations of m and n , in total $2 \times 2 \times 6 \times 2 = 48$ different TOF offsets O_T need to be considered. However, for some parameter combinations, there are very few measurements left (less than 100), having taken into account equation (3). In these cases, we abstain from computing O_T and disregard measurements of the respective modes for the following TOF method computations. For all other parameter combinations, TOF offsets O_T and uncertainties ΔO_T are listed in table 1.

For step 2, assumptions with respect to Δg and ΔB_n are required. Orthogonalization angles and gains (matrices G and M) are assumed to be accurate to the order $\Delta g = 10^{-4}$. The noise level of the Cluster FGMs is on the order of $\Delta B_n = 10\,\text{pT}$. Therewith, we obtain uncertainties ΔO_x via equation (11). They are color coded in figure 2 and depicted as a function of $|B|$ and the angle ξ_B (blue in figure 1) between B and the spin axis x . As expected, the uncertainties ΔO_x decrease with $|B|$ and ξ_B . Hence, low ΔO_x are found in the lower left corner of that figure.

The value of $\Delta g = 10^{-4}$ reflects the order of magnitude of long term variations of those calibration parameters, influencing G and M , that can be accurately determined in flight (e.g. the ratio of the spin plane component gains). However, some calibration parameters that influence $|B|$, as measured by the FGM, namely the absolute spin axis and spin plane gains, cannot be easily and/or accurately determined in flight. It has to be assumed, without possibility of verification, that their long term variations are of the same order of magnitude. Consequently, FGM measurements are not guaranteed to exhibit relative accuracies on the order of or better than

$\Delta g = 10^{-4}$. Nevertheless, for the purpose of spin axis offset determination, we necessarily have to assume that the only undetermined calibration parameter is, indeed, O_x .

In step 3, we compute O_{xf} for sliding windows of $t_{\text{int}} = 15\,\text{min}$ shifted by 5 min. The quality thresholds were set to $C_O = 0.2\,\text{nT}$ and $C_\# = 100$, respectively. Therewith, we obtain 3523 final offset correction values O_{xf} distributed over 68 different orbits. The distribution of O_{xf} values is depicted by a red line in figure 3(c).

The figure illustrates how a number of EDI measurements per orbit (panel (a)) taken at certain $|B|$ conditions (panel (b)) is converted into a number of final offset correction values O_{xf} (red line, panel (c)). Interestingly, O_{xf} values were computed roughly for every second orbit. This can be easily explained: For O_{xf} computations, we selected O_x estimates that fulfill $\Delta O_x \leq C_O = 0.2\,\text{nT}$. As shown in figure 2, these estimates are obtained in significant numbers for magnetic field strengths below 60 nT. EDI measurements in this field range were taken roughly during every second orbit (see figure 3(b)). For those orbits, O_{xf} values are computed.

3.2. BD method

Each GDU can emit electrons in a solid angle range larger than 2π around a central axis. On Cluster, this axis is perpendicular to the spin axis. For convenience, we assume it to point in z -direction. For angles ζ_D between D and z (shown in green in figure 1) approaching or even surpassing 90° , the beam width is known to increase significantly. This effect would deteriorate the results of the BD method. Therefore, we exclude EDI measurements with $\zeta_D > C_D = 80^\circ$.

For the coordinate system adjustment (step 1 of the BD method) we select EDI (and corresponding FGM) measurements for which $D_x < C_{\text{sp}} = 0.1$ holds (equation (15)). Minimal deviations on the order of 0.6° are found between the coordinate system transformations that are obtained from EDI/FGM data comparison and the nominal transformations that are given by the Cluster spacecraft building plans. The angular uncertainties of the former transformations are $\Delta\beta = 0.25^\circ$ for GDU 1 and $\Delta\beta = 0.28^\circ$ for GDU 2.

Again, we assume $\Delta g = 10^{-4}$ and $\Delta B_n = 10\,\text{pT}$. The resulting uncertainties ΔO_x are shown in figure 4, this time as a function of $|B|$ and the angle ξ_D between D and the spin axis x (depicted in red in figure 1). Figure 4 is somewhat similar to figure 2 as lower uncertainties ΔO_x are also found in the lower left corner, corresponding to lower field values $|B|$ and lower angles ξ_D (i.e. D close to the spin axis). However, for equal field values $|B|$ minimal uncertainties ΔO_x are larger for the BD method than for the TOF method.

The final offset correction values O_{xf} are computed for $t_{\text{int}} = 15\,\text{min}$ sliding windows shifted by 5 min, $C_O = 0.2\,\text{nT}$, and $C_\# = 100$. Therewith we obtain 2792 values O_{xf} distributed over 46 orbits. The numbers of these values per orbit are depicted in figure 3(c) by green bars.

3.3. SW method

In 2008, the apogee distances of Cluster 3 to the Earth's center were larger than 20 Earth radii. Hence, dayside apogee positions

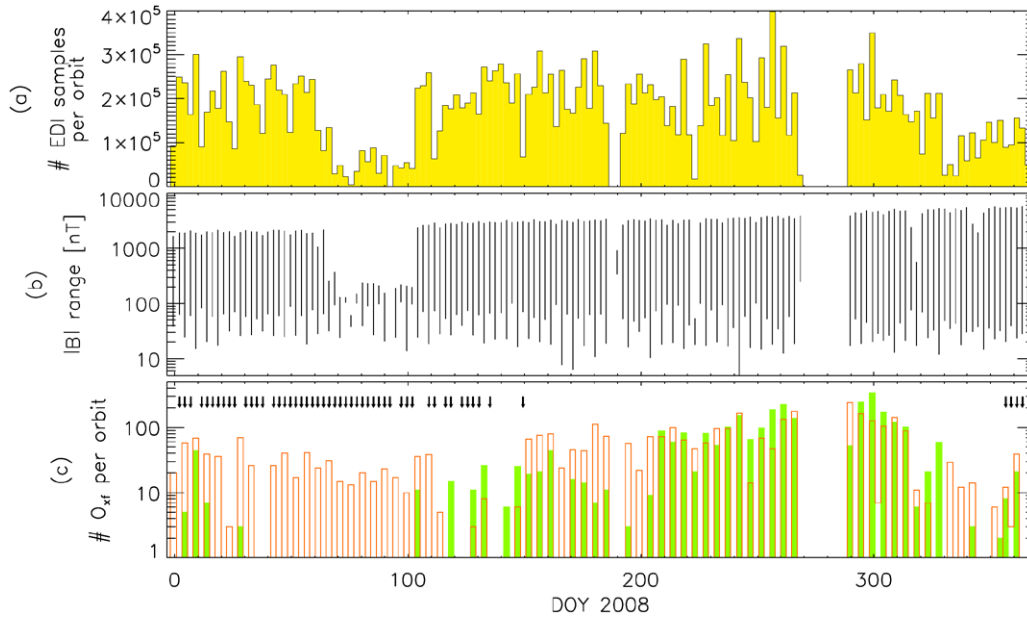


Figure 3. (a) Numbers of EDI samples (i.e. BD and TOF measurements) per orbit. (b) Lines connect minimum and maximum $|B|$ values corresponding to EDI measurements. (c) Numbers of values O_{xf} per orbit as obtained by the TOF method (red lines) and by the BD method (green bars). Orbits for which a spin axis offset could be determined by the SW method are marked by black arrows.

were beyond the bow shock, in the pristine solar wind (SW). Due to the Earth's rotation around the Sun, the apogee positions rotated once around Earth over the course of the year. When they were at the night side, Cluster 3 stayed inside the magnetosphere and the SW was not observed. Consequently, SW measurements were performed by Cluster 3 not during the entire year, but are available just for the first 6 months and for December of 2008.

We applied the SW method to the solar wind (spin averaged) FGM measurements of each orbit, if available. Specifically, we used the parameters and criteria given in the 'THEMIS' column of table 1 of [13]. As a result, we obtained 53 spin axis offset corrections O_{xf} pertaining to 53 different orbits (49 for DOYs 2–150, and 4 for DOYs 357–364). The corresponding solar wind data intervals ranged between 32 and 57 h in length. Orbits for which a final spin axis offset correction O_{xf} could be computed by the SW method are marked by black arrows in figure 3(c).

4. Results and discussion

The O_{xf} results of the three methods are shown in figure 5(a) (red dots: TOF method, green dots: BD method, black crosses: SW method). In total, 6368 O_{xf} values contribute to that figure: 3523 from the TOF method, 2792 from the BD method, and only 53 from SW method. The results show consistently that the spin axis offset (as part of the FGM calibration files for that year) is, in general, off by about -0.2 nT. This systematic deviation is expected as the spin axis offset value in the calibration files for 2008 was determined in 2003. Since then, the offset has been checked periodically, but has been kept constant, as its changes were found to lie within its margins of error (Fornaçon, personal communication). Consequently, deviations of O_{xf} from 0 reflect the long term offset drift in spin axis direction from 2003 to 2008.

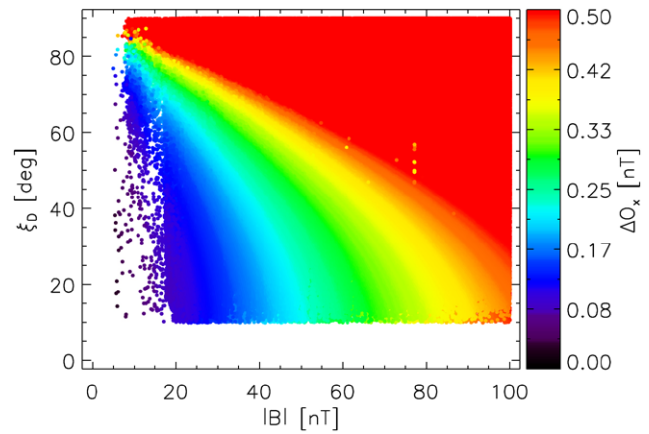


Figure 4. ΔO_x , resulting from the application of the BD method to Cluster 3 EDI and FGM measurements from 2008, as a function of $|B|$ and the angle ξ_D between \mathbf{D} and the spin axis x . Note that EDI measurements with $\xi_D < 10^\circ$ are excluded, as they also fulfill $\xi_D > C_D = 80^\circ$ (see figure 1).

Median values of O_{xf} are -0.20 nT (TOF method), -0.15 nT (BD method), and -0.26 nT (SW method). The corresponding standard deviations are 0.11 nT, 0.08 nT and 0.15 nT, respectively. Taking into account these standard deviations, in particular of the SW method results, we have to regard the median spin axis offset corrections resulting from the three methods as quantitatively similar.

The average errors $\langle \Delta O_{xf} \rangle$ (after equation (14)) of all O_{xf} values are depicted in figure 5(b). The minima and maxima of this quantity are 0.05 and 0.53 nT (TOF method), 0.06 and 0.59 nT (BD method), as well as 0.04 and 0.32 nT (SW method). The medians of $\langle \Delta O_{xf} \rangle$, which are more representative of the typical uncertainties, are 0.14 , 0.12 and 0.12 nT for the TOF, BD, and SW method offsets, respectively. Hence, they are practically equal. If the margins of error of the results

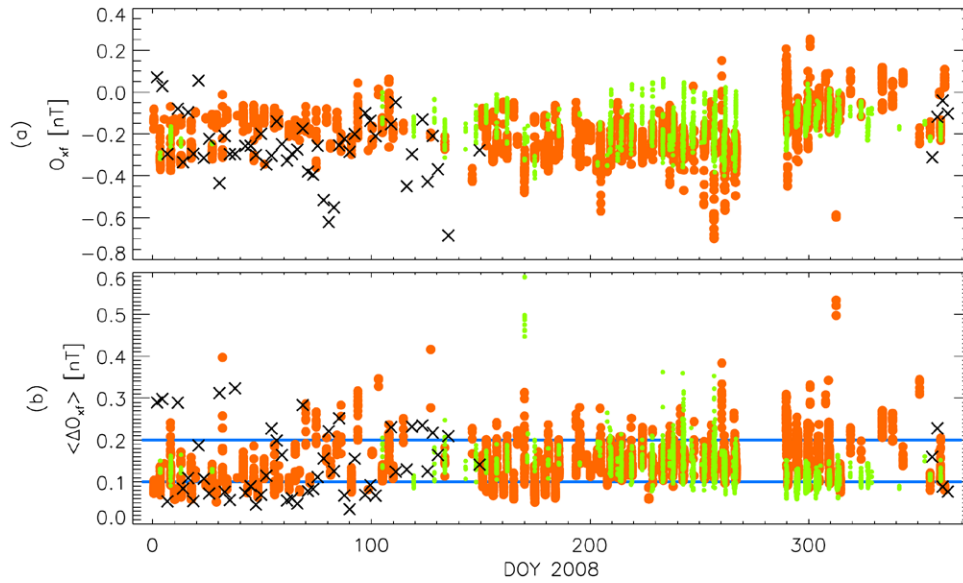


Figure 5. (a) Final spin axis offset corrections O_{xf} obtained by the TOF method (red dots), the BD method (green dots), and the SW method (black crosses). (b) Corresponding average errors $\langle \Delta O_{xf} \rangle$ after equation (14). The blue lines mark $\langle \Delta O_{xf} \rangle = 0.1$ nT and 0.2 nT levels (see text for details).

from the different methods are associated with similar statistical confidence levels, then the accuracies of the results obtained with the three methods will be practically equal, on average, as well.

The blue lines in figure 5(b) mark levels of uncertainty of $\langle \Delta O_{xf} \rangle = 0.1$ nT and 0.2 nT. These levels correspond with two MMS mission requirements: 0.1 nT and 0.2 nT are the desired and minimum accuracy goals for FGM magnetic field measurements (referring to $|\mathbf{B}_{\text{measured}} - \mathbf{B}_{\text{true}}|$), to be achieved by the MMS spacecraft in science target (i.e. reconnection) regions e.g. [22]. The figure suggests that $\langle \Delta O_{xf} \rangle \leq 0.1$ nT is achievable by all three methods.

It has to be pointed out that this conclusion is only valid if the calibration parameters other than the spin axis offset, in particular those parameters pertaining to the matrices \mathbf{G} and \mathbf{M} , are known with sufficient accuracy. Here, we assume relative uncertainties on the order of $\Delta g = 10^{-4}$ in equation (10), which result in small FGM measurement errors on the order of 10 pT for fields of 100 nT. Uncertainties of (much) higher order of magnitude in \mathbf{G} and \mathbf{M} , however, may noticeably alter the outcome of the spin axis offset correction estimates O_x and, consequently, of O_{xf} , without necessarily increasing $\langle \Delta O_{xf} \rangle$.

Numbers of O_{xf} values from the TOF and BD methods that (nominally) fulfill the accuracy criteria with respect to $\langle \Delta O_{xf} \rangle$ are given in table 2; the offsets are distributed over certain numbers of orbits that are given in brackets (maximum: 73 orbits, for which there are TOF and/or BD method offset corrections O_{xf}).

O_{xf} with $\langle \Delta O_{xf} \rangle \leq 0.2$ nT are obtained for 70 out of 73 orbits. If the stricter criterion of $\langle \Delta O_{xf} \rangle \leq 0.1$ nT is used, corresponding offsets are still obtained for 46 out of 73 orbits. Interestingly, only for 8 of these 46 orbits there are sufficiently accurate O_{xf} values from both TOF and BD methods. For the other 38 orbits, either TOF or BD method offsets are obtained with sufficient accuracy. This finding is an indication of the complementarity of the methods.

Table 2. Numbers of offset corrections O_{xf} from the TOF method, the BD method, and both methods fulfilling $\langle \Delta O_{xf} \rangle \leq 0.1$ nT and $\langle \Delta O_{xf} \rangle \leq 0.2$ nT, respectively. Numbers of orbits over which the offset corrections are distributed are given in brackets. The total number of orbits for which TOF and/or BD method O_{xf} are available is 73.

	Numbers of offset corrections (orbits)		
	TOF method	BD method	TOF and BD methods
$\langle \Delta O_{xf} \rangle \leq 0.1$ nT	496 (34)	594 (20)	1090 (46)
$\langle \Delta O_{xf} \rangle \leq 0.2$ nT	3106 (64)	2674 (46)	5780 (70)

Obviously, the SW method is complementary to the TOF and BD methods, as it is dependent on measurements in the solar wind. EDI, instead, does not work in the solar wind, as typical magnetic field strengths there (of a few nT) are too low for operation. This can be seen in figures 2 and 4, which show only few measurements below $|\mathbf{B}| = 10$ nT.

It should be noted that the low magnetic field strengths in the solar wind relax the requirement for accurate knowledge of the matrices \mathbf{G} and \mathbf{M} prior to spin axis offset determination with the SW method, because the measurement uncertainties associated to \mathbf{G} and \mathbf{M} scale with $|\mathbf{B}|$ (the factor being given by Δg , see equation (10)).

Although the TOF and BD methods are both based on EDI measurements, they are also complementary to each other. The reason is rooted in the perpendicularity of \mathbf{D} and \mathbf{B} . Most accurate O_x estimates are obtained with the TOF method if \mathbf{B} is close to the spin axis (small angle ξ_B , see figure 2). For the BD method, it is more favorable if \mathbf{D} is closer to the spin axis (small angle ξ_D , see figure 4). As a matter of fact, for $\xi_B < \tilde{\xi}$ where $\tilde{\xi}$ is an arbitrary angle between 0° and 90° , $\xi_D > 90^\circ - \tilde{\xi}$ necessarily follows (and vice versa; see figure 1). Consequently, EDI and simultaneous FGM measurements tend to be either favorable for the TOF or for the BD method, but cannot be perfect for both.

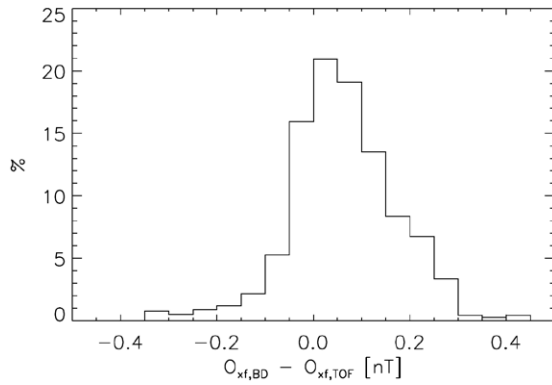


Figure 6. Distribution of differences $O_{xf,BD} - O_{xf,TOF}$ for simultaneous offset results from both methods.

Nevertheless, for observations in low $|B|$, there is an overlap in EDI/FGM measurements of acceptable quality for both methods (e.g. $\Delta O_x < C_O = 0.2$ nT, see figures 2 and 4). These measurements result in simultaneous O_{xf} values from both TOF and BD methods, which we can directly compare. Figure 6 shows the distribution of differences of the 1162 simultaneous BD and TOF O_{xf} results. As can be seen, differences between the two methods are minor on average: the mean and median of the distribution is 0.06 nT. Hence, BD method-determined O_{xf} tend to be slightly higher than those determined with the TOF method. The standard deviation of the distribution, however, is 0.11 nT, i.e. about twice as large as the mean and median values of the distribution. Hence, average, systematic differences between TOF and BD method O_{xf} results are small in comparison to the width of the distribution.

Furthermore, from the 1162 simultaneous offsets, 1130 BD method O_{xf} are within the corresponding TOF method error margins, i.e. between $O_{xf} - \Delta O_{xf-}$ and $O_{xf} + \Delta O_{xf+}$. Conversely, 905 TOF method O_{xf} values are within the error margins of the corresponding BD method offsets. Also in that respect, O_{xf} results from both methods have to be regarded as quantitatively similar.

As discussed above, a comparison of simultaneous O_{xf} values resulting from the SW method and from the TOF or BD methods is impossible due to the complementarity of the methods. In the next best case, O_{xf} values from either the TOF or the BD method are available before and after an O_{xf} estimate by the SW method within a common orbit. This is the case for 13 orbits (see dates on the vertical axis of figure 7). Spin axis offset corrections were obtained by the TOF method during both outbound and inbound passes of Cluster 3 through the magnetosphere on those orbits. SW method O_{xf} values are based on the solar wind intervals in between, around apogees. For each of those orbits, we linearly interpolate TOF method O_{xf} values and error bounds ($O_{xf} + \Delta O_{xf+}$ and $O_{xf} - \Delta O_{xf-}$) to the central times of the solar wind intervals that the SW method has been applied to. The interpolates are shown in figure 7 in red. The corresponding SW method results are depicted in black.

In eight cases the SW method results are within the margins of error of the TOF method offset corrections (and vice versa).

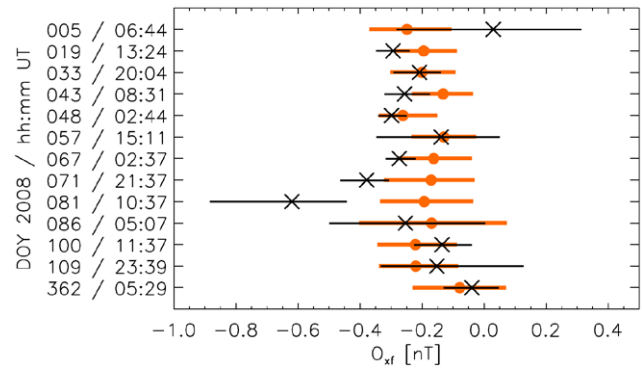


Figure 7. Black crosses and lines: O_{xf} results from the SW method and corresponding margins of error between $O_{xf} + \Delta O_{xf+}$ and $O_{xf} - \Delta O_{xf-}$. Corresponding interpolated TOF method results are depicted by red dots and lines.

Furthermore, the margins of error overlap in 12 out of 13 cases (exception: DOY 81). The mean O_{xf} values are -0.23 nT (SW method) and -0.18 nT (TOF method); they are quite similar to the results obtained for the entire year 2008. As can be seen, the TOF method-determined offsets are much more stable; this is reflected in the respective standard deviations of 0.16 nT (SW method) and 0.05 nT (TOF method). The relative stability of the TOF method results suggests that they may be more accurate than the SW method results.

The relative stability of the TOF method results is surprising when taking into account that the TOF method results are based on data from relatively short periods of time ($t_{int} = 15$ min intervals). The SW method O_{xf} estimates, instead, are based on solar wind data intervals that are more than one day long. Consequently, we would expect the SW method-based offset corrections to be more time-averaged and, hence, stable than the TOF method results, contrary to our findings.

5. Summary and conclusions

In this paper, we improve the time-of-flight (TOF) method for FGM spin axis offset determination by using a comprehensive error analysis. It allows for the selection of the most accurate offset (correction) estimates O_x for the computations of final spin axis offsets (or offset corrections) O_{xf} . Furthermore, we introduce a new method for the same task, denoted as beam direction (BD) method, that is complementary to the TOF method. While both are based on the comparison of EDI and simultaneous FGM measurements, the TOF method benefits from low angles ξ_B and the BD method from low angles ξ_D . Both conditions are mutually exclusive. Under low magnetic field conditions, the two methods allow for computations of O_{xf} independently of the ambient magnetic field direction with respect to the spin axis of the observing spacecraft.

In addition, the error analysis enables us to sensibly choose among TOF and BD method results, when both are available. In fact, it facilitates the combination of both methods after their respective steps 2: O_x estimates and the corresponding uncertainties ΔO_x may be merged into a single data set. The increased sample size would improve the

statistical basis of the final results O_{xf} or allow for lowering C_O and/or increasing $C_\#$.

Furthermore, we compare the results of the TOF and BD methods with those from a typically used SW method. These are our findings:

- In general, the offset correction results for the considered Cluster 3 FGM data from 2008, obtained with the three methods, tend to lie consistently around -0.2 nT.
- Standard deviations of the results of either of the three methods are on the order of 0.1 nT. Systematic differences between results from different methods are equal or smaller.
- Errors $\langle \Delta O_{xf} \rangle$ are typically a little larger, yet very similar among the three methods: around 0.13 nT, on average.
- O_{xf} values from the TOF or BD methods are mostly included in the error margins of the corresponding O_{xf} estimates from the respectively other method. This further indicates that the TOF and BD method results are quantitatively very similar.
- The comparison of the TOF and SW method results shows that the latter seem to be less stable, in contrast to expectations. This finding suggests (without proof) that the TOF method results are more accurate than the SW method ones.

Altogether, we find the TOF and BD methods to perform similarly well, while the SW method results may be equally or slightly less accurate. Furthermore, the TOF and BD methods are able to provide O_{xf} estimates with much higher cadence (we used $t_{\text{int}} = 15$ min). Instead, the SW method requires solar wind data intervals that are at least several hours long [13]. On the other hand, the TOF and BD methods rely more than the SW method on the accurate knowledge of calibration parameters other than the spin axis offset.

Finally, we approach the question of how readily usable the TOF and BD methods are for routine FGM spin axis offset calibration, in reference to the upcoming MMS mission. We find that most accurate offset estimates are obtained from EDI and FGM measurements in low magnetic field regions. Magnetospheric field strengths per orbit observed by MMS are expected to be highest in the subsolar region. There, field strengths of $|\mathbf{B}| \approx 50$ nT are typical, just Earthward of the magnetopause. Even under these (worst case) conditions, accurate O_x estimates can be provided at least by the TOF method, likely also by the BD method over a wide range of angles ξ_B and ξ_D (see figures 2 and 4). Furthermore, we find that both methods are able to yield O_{xf} values with (the required) accuracies of $\langle \Delta O_{xf} \rangle \leq 0.1$ nT or 0.2 nT. Offsets (or, more precisely, offset corrections) fulfilling the latter condition are distributed over almost all orbits for which EDI measurements in low magnetic field regions are available. Hence, we can conclude that the TOF and BD methods, introduced herein,

constitute working EDI-based methods that are suitable for routine FGM spin axis offset calibration. This applies in particular to the MMS flux-gate magnetometers, but is dependent on the precise knowledge of the other calibration parameters.

Acknowledgments

We thank the Cluster Active Archive (CAA) team and, in particular, C Carr and R Torbert for the use of Cluster FGM, EDI, and supplementary data. Furthermore, we thank K-H Glassmeier and K-H Fornacon for the use of Cluster FGM daily calibration files and pertaining FGM data processing software, as well as for valuable discussions on the process of generation and accuracy of the daily calibration files. This research was partly supported by the Austrian Science Fund (FWF): I429-N16.

References

- [1] Acuña M H 2002 *Rev. Sci. Instrum.* **73** 3717–36
- [2] Auster H U, Fornacon K H, Georgescu E, Glassmeier K H and Motschmann U 2002 *Meas. Sci. Technol.* **13** 1124–31
- [3] Auster H U et al 2008 *Space Sci. Rev.* **141** 235–64
- [4] Balogh A 2010 *Space Sci. Rev.* **152** 23–97
- [5] Belcher J W 1973 *J. Geophys. Res.* **78** 6480–90
- [6] Davis L Jr and Smith E J 1968 *Eos Trans. AGU* **49** 257
- [7] Fornacon K H, Georgescu E, Kempen R and Constantinescu D 2011 Fluxgate magnetometer data processing for Cluster *Technical Report* Institut für Geophysik und extraterrestrische Physik, Technische Universität Braunschweig, Braunschweig, Germany
- [8] Georgescu E et al 2006 *Cluster and Double Star Symposium* ESA Special Publication vol 598 (Noordwijk: ESA)
- [9] Glassmeier K H et al 2007 *Space Sci. Rev.* **128** 649–70
- [10] Hedgecock P C 1975 *Space Sci. Instrum.* **1** 83–90
- [11] Kepko E L, Khurana K K, Kivelson M G, Elphic R C and Russell C T 1996 *IEEE Trans. Magn.* **32** 377–85
- [12] Leinweber H K, Russell C T and Torkar K 2012 *Meas. Sci. Technol.* **23** 105003
- [13] Leinweber H K, Russell C T, Torkar K, Zhang T L and Angelopoulos V 2008 *Meas. Sci. Technol.* **19** 055104
- [14] Ludlam M et al 2008 *Space Sci. Rev.* **141** 171–84
- [15] Nakamura R et al 2014 *Geosci. Instrum. Methods Data Syst.* **3** 1–1
- [16] Ness N F, Scarce C S and Seek J B 1964 *J. Geophys. Res.* **69** 3531–69
- [17] Paschmann G et al 1997 *Space Sci. Rev.* **79** 233–69
- [18] Pudney M A, Carr C M, Schwartz S J and Howarth S I 2012 *Geosci. Instrum. Methods Data Syst.* **1** 103–9
- [19] Quinn J M et al 1999 *Ann. Geophys.* **17** 1503–12
- [20] Rosenberg R L 1971 *Automatic Calculation of Zero Levels for Interplanetary Spacecraft Magnetometers by the Davis Method* Publ. No. 903, Institute of Geophysics and Planetary Physics, University of California Los Angeles
- [21] Russell C T et al 2014 *Space Sci. Rev.* online, doi:10.1007/s11214-014-0057-3
- [22] Torbert R B et al 2014 *Space Sci. Rev.* submitted